

# Effect of Chalcogens on Electronic and Photophysical Properties of Vinylene-Based Diketopyrrolopyrrole Copolymers

Joydeep Dhar,<sup>†</sup> Tushita Mukhopadhyay,<sup>†</sup> Nir Yaacobi-Gross,<sup>‡</sup> Thomas D. Anthopoulos,<sup>‡</sup> Ulrike Salzner,<sup>§</sup> Sufal Swaraj,<sup>||</sup> and Satish Patil<sup>\*†</sup>

<sup>†</sup>Solid State and Structural Chemistry Unit, Indian Institute of Science, Bangalore 560012, India

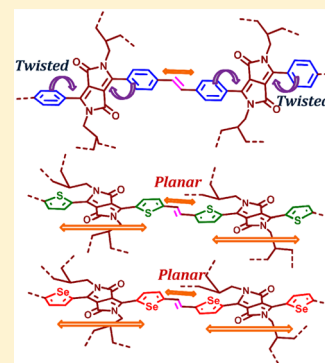
<sup>‡</sup>Department of Physics and Centre for Plastic Electronics, Blackett Laboratory, Imperial College London, London 7W72BW, U.K.

<sup>§</sup>Department of Chemistry, Bilkent University, 06800 Bilkent, Ankara, Turkey

<sup>||</sup>Synchrotron SOLEIL, L'Orme des Merisiers Saint-Aubin - BP 48, F-91192 Gif-sur-Yvette Cedex, France

## S Supporting Information

**ABSTRACT:** Three vinylene linked diketopyrrolopyrrole based donor–acceptor (D–A) copolymers have been synthesized with phenyl, thienyl, and selenyl units as donors. Optical and electronic properties were investigated with UV–vis absorption spectroscopy, cyclic voltammetry, near edge X-ray absorption spectroscopy, organic field effect transistor (OFET) measurements, and density functional theory (DFT) calculations. Optical and electrochemical band gaps decrease in the order phenyl, thienyl, and selenyl. Only phenyl-based polymers are nonplanar, but the main contributor to the larger band gap is electronic, not structural effects. Thienyl and selenyl polymers exhibit ambipolar charge transport but with higher hole than electron mobility. Experimental and theoretical results predict the selenyl system to have the best transport properties, but OFET measurements prove the thienyl system to be superior with p-channel mobility as high as  $0.1 \text{ cm}^2 \text{ V}^{-1} \text{ s}^{-1}$ .



## 1. INTRODUCTION

Polyene based  $\pi$ -conjugated polymers poly(phenylenevinylene) (PPV) are among the most well-studied organic semiconductors, synthesized in the early developing years of  $\pi$ -conjugated polymers.<sup>1</sup> PPV has received much attention as a material of choice for organic light-emitting diodes (OLEDs) due to its high luminescence.<sup>1–3</sup> To improve solubility as well as to tune its functionalities, the chemical structures were further modulated by changing the alkyl groups attached to the phenyl rings to have a range of vinylene based polymeric semiconductors.<sup>4,5</sup> Variation at the core with different aromatic groups in conjugation with a vinylene unit has led to the multitude of combinations.<sup>6,7</sup> Poly(thienylenevinylene) (PTV) and its selenium analogue poly(selenylenevinylene) (PSV), the simplest vinylene based polymers, were developed later.<sup>8,9</sup> PTV showed improved electrical performances.<sup>10–13</sup> Moreover, recent findings have demonstrated that this material can exhibit singlet fission foreshadowing bright prospects for photovoltaic applications because it improves power conversion efficiencies.<sup>14</sup> However, the non-centrosymmetric alkyl chain attached to the thiophene ring in PTV gives rise to the regiorandomness and causes structural defects limiting charge transport properties.<sup>15</sup> Until now, various synthetic strategies have been adopted to minimize the drawback related to the structural disorder<sup>16–19</sup> and accordingly device performances have been improved with the regioregular polymers.<sup>4</sup> Extensive experimental and theoretical studies on vinylene polymers have revealed that, in addition to the structural disorder, conforma-

tional disorder also has a strong influence on the device outcome.<sup>20</sup> A twist or bent of the polymer chain leads to the conformational defects, which limit the conjugation length and localize the charge carrier between two defect states.<sup>20–22</sup> Therefore, a polymer chain may consist of multiple chromophoric segments controlling the overall intra- and interchain charge transfer processes.<sup>23</sup> Such defects severely affect the charge carrier energetic and transport properties of the polymeric backbone. In polyenes, the presence of *cis*-defects or tetrahedral carbons are sources of conformational disorder<sup>22,24</sup> which is proved to be detrimental for device applications. There is an ongoing effort to control the conformational defects arising during polymer synthesis or while processing to achieve optimal electronic and optical properties.<sup>25</sup> Hence, it is crucial to understand the origin and identify the nature of such defect states to avoid limitations of polyene based donor–acceptor conjugated polymers.

In the field of  $\pi$ -conjugated organic materials, diketopyrrolopyrrole (DPP) has emerged as a versatile chromophore. Due to its ideal chemical and electronic structure, DPP based materials have added new dimensions both in organic photovoltaics (OPVs) and organic field effect transistor

**Special Issue:** Biman Bagchi Festschrift

**Received:** April 1, 2015

**Revised:** May 18, 2015

**Published:** June 8, 2015

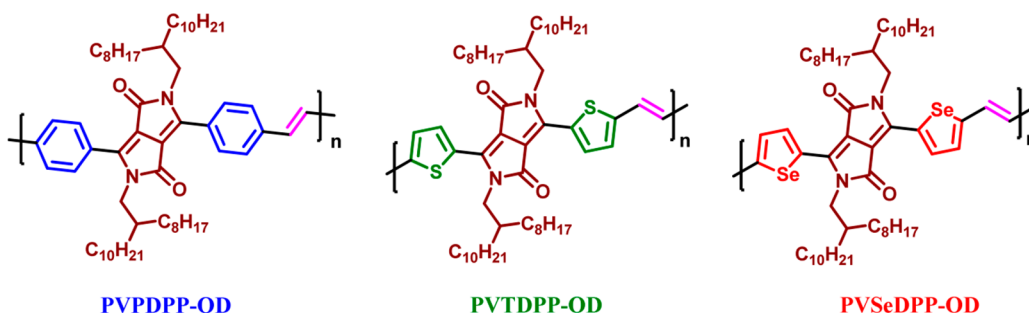
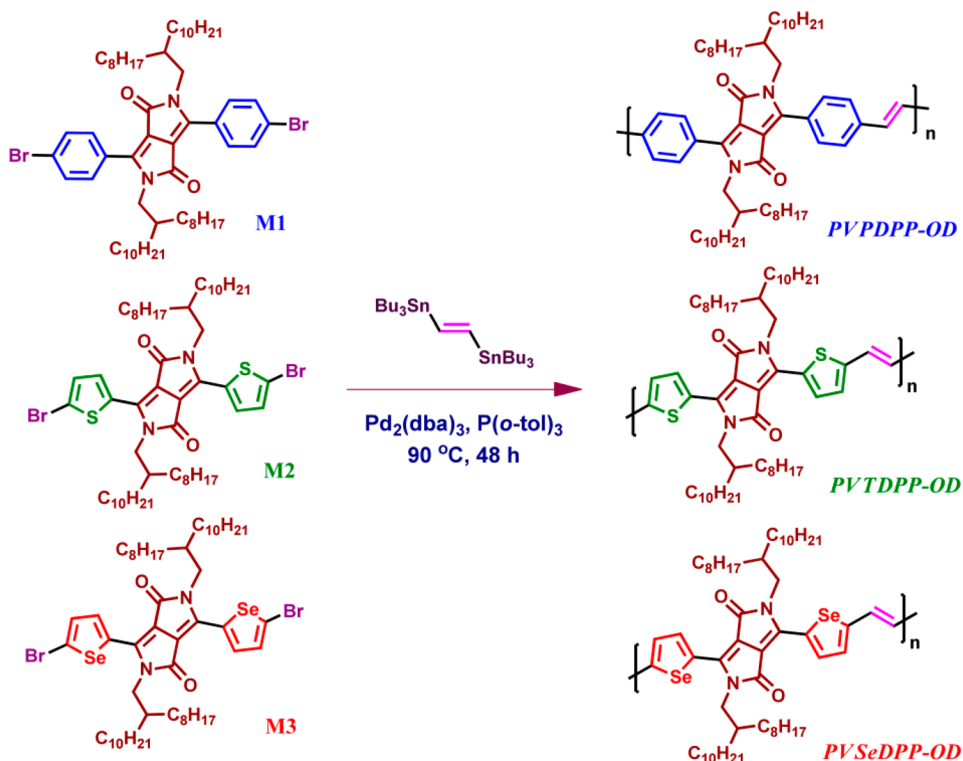


**Figure 1.** Chemical structure of three vinylene DPP based copolymers.

**Scheme 1.** Synthesis of Three Vinylene DPP Based Copolymers



(OFET) devices.<sup>26–35</sup> Recently, Jenekhe and co-workers have reported two vinylene-based DPP copolymers synthesized in conjugation with thienyl and phenyl coupled DPP units. Among them, thienyl based polymer has demonstrated an efficient ambipolar characteristic as compared to its phenyl analogue due to favorable electronic and structural properties.<sup>36</sup> Yun et al. have shown that the performance of vinylene based materials is highly susceptible to the chain conformation next to the vinylene unit.<sup>37</sup> Thiophene coupled DPP polymers with the vinylene linkage showed enhanced charge transport properties.<sup>38–41</sup> Kim and co-workers have demonstrated that charge carrier mobility in a vinylene linked thiophene DPP based copolymer can be improved with the substitution of selenophene.<sup>28,42,43</sup> Recently, the nature (p- and n-type) of the charge transport property was finely tuned by attaching a strong electron withdrawing group at the vinylene linkage in a DPP based copolymer.<sup>44,45</sup> Thus, the variety of results obtained for vinylene systems reveals that a clear and conclusive understanding is lacking about the role of the vinylene moiety in organic semiconductors. In the present work, we have carried out a comparative study on three vinylene-based DPP donor–

acceptor (D–A) copolymers, designated as PVPDPP-OD, PVTDPP-OD, and PVSeDPP-OD. The chemical structures of the three copolymers are shown in Figure 1. The comparative study of the three polymers reflects the influence of the donor groups on the electronic properties in a  $\pi$ -conjugated organic framework. Theoretical calculations were performed on oligomers of increasing length to analyze the underlying reasons for the different electronic properties. Comparison of theoretical results with photophysical and charge transport properties allows separating the influence of electronic differences from that of torsional disorder in the backbone of the three polymers.

## 2. RESULTS AND DISCUSSION

**2.1. Synthesis and Characterization.** All the monomers were synthesized according to previously reported literature methods. The three different DPP based chromophores, i.e., PDPP, TDPP, and SeDPP, were synthesized by a *pseudo*-Stobbe condensation reaction between isopropyl succinic ester and *p*-bromo benzonitrile or 2-thiophene carbonitrile or 2-selenophene carbonitrile in the presence of a strong base

sodium *tert*-amyl alkoxide.<sup>46</sup> Synthesis of the three copolymers PVPDPP-OD, PVTDPP-OD, and PVSeDPP-OD is shown in Scheme 1. These polymers were synthesized by a Stille coupling reaction between monomer M1 or M2 or M3 and *trans*-1,2-bis(tributylstannyl)ethylene in the presence of a palladium catalyst Pd<sub>2</sub>(dba)<sub>3</sub> with ligand P(*o*-tol)<sub>3</sub> in a Schlenk tube. The reaction mixture from the Schlenk tube was precipitated into methanol, and crude polymer was purified through Soxhlet extraction in methanol and acetone.

The average molecular weights of the synthesized polymers were determined by gel permeation chromatography (GPC) using THF as an eluent against the polystyrene standard. Polymers with their number-average molecular weight ( $M_n$ ), weight-average molecular weight ( $M_w$ ), and polydispersity index (PDI) are given in Table 1. These polymers are highly

**Table 1. Molecular Weight Distribution of the Three Copolymers**

polymer	molecular weight		PDI
	$M_n$ (kg/mol)	$M_w$ (kg/mol)	
PVPDPP-OD	25.6	48.3	1.89
PVTDPP-OD	15.6	38.8	2.49
PVSeDPP-OD	14.1	32.5	2.3

soluble in common organic solvents such as chloroform, chlorobenzene, and tetrahydrofuran (THF) at room temperature. Structural characterization of the monomers and polymers was carried out using <sup>1</sup>H and <sup>13</sup>C NMR spectroscopy.

**2.2. Photophysical Properties.** Optical properties of the three vinylene-based polymers were characterized by UV–visible spectroscopy. All three polymers exhibit dual band absorption in their UV–visible spectra (Figure 2), but

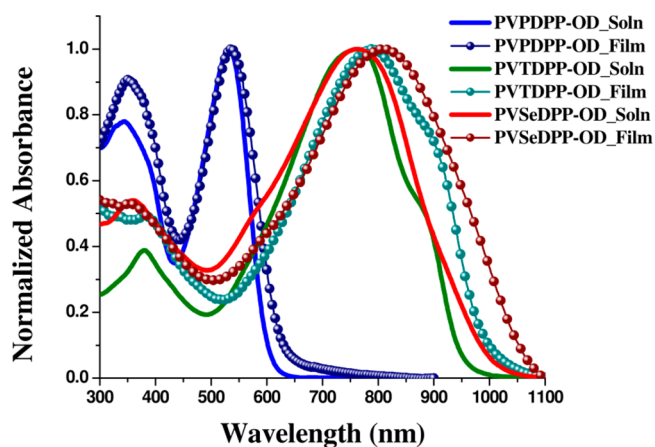


**Figure 2.** Normalized absorption spectra of three DPP based vinylene copolymers in ODCB and in thin film.

significant differences are observed in their absorption spectra by changing the donor group attached to the DPP unit. The low energy peak gradually shifts red from PDPP to SeDPP polymers, 530 nm for PVPDPP-OD, 762 and 765 nm for PVTDPP-OD and PVSeDPP-OD, respectively. Previously, it has been claimed that hydrogen–hydrogen steric repulsion leads to the torsion of the phenyl ring in PDPP, resulting in poor intermolecular electronic coupling between donor and acceptor units.<sup>46,47</sup> Another possible reason for the higher absorption energy of PVPDPP is the high aromatic resonance

stabilization energy of the phenyl group, rendering phenyl a weaker donor than thienyl and selenyl moieties.<sup>46</sup> Theoretical analysis shown below indicates that differences in electronic properties contribute more than twisting to the difference in absorption energies. In thin films, the corresponding peak maxima are bathochromically shifted to 536, 788, and 809 nm for PVPDPP-OD, PVTDPP-OD, and PVSeDPP-OD. The broader absorption spectrum with a greater red shift of 44 nm for PVSeDPP-OD compared to 26 nm for PVTDPP-OD in the thin film absorption spectra indicates the presence of stronger intermolecular interaction for selenium-based polymers. The intense high-energy transition in PDPP based polymers implies poor electronic coupling between the donor and acceptor unit in the polymer backbone. The ratio of the low- to high-energy band decreases in going from solution to the solid state for PVPDPP-OD and PVTDPP-OD, but the ratio remains almost the same for the selenium-based polymers. This observation suggests that the effect of conformational disorder is least for PVSeDPP-OD, as reflected in its absorption spectra.

The vibronic feature in the low energy absorption band for PVTDPP-OD indicates the presence of interchain aggregates due to its low solubility in the solution, and this characteristic becomes more pronounced in the thin film. The absorption-edge optical band gaps of PVTDPP-OD and PVSeDPP-OD are comparable and measured to be 1.29 and 1.28 eV, respectively. The band gap of PVPDPP-OD is wider, 2.06 eV. Compared to the band gaps of DPP polymers without a vinylene linkage (e.g., 2DPP-OD-OD,  $\Delta E_g = 1.22$  eV), which were previously reported by our group,<sup>48</sup> the optical band gap increases due to inclusion of the vinylene unit in the polymer backbone.<sup>48</sup>

**2.3. Theoretical Calculations.** To analyze the electronic structures of PVPDPP-OD, PVTDPP-OD, and PVSeDPP-OD, dimers, trimers, and tetramers of VPDPP, VTDPP, and VSeDPP were investigated at the B3P86-30%/6-31g\* level of theory. The 2-octyldecyl chains that do not contribute to the electronic properties of the isolated molecules were replaced by methyl groups to reduce the computing time.

Figure 3 shows the absorption spectra of tetramers calculated with time-dependent density functional theory. Like in the experimental spectra, 4-VTDPP and 4-VSeDPP exhibit a strong low energy band and weak absorptions around 400 nm. The first band of 4-VPDPP occurs at a much higher energy than that of the other two systems and is weaker. In contrast, the high-energy band is stronger. Compared to experiment, the oscillator strengths of the high-energy features may be somewhat underestimated, which would be the case in the presence of some structural disorder in the experiment.

Excitation energies of oligomers are summarized in Table 2. For comparison with experiment, oligomer data were extrapolated with second degree polynomial fits to the approximate experimentally determined chain lengths (31 units for VPDPP, 19 units for VTDPP, and 15 units for VSeDPP) obtained by dividing the average molecular weights  $M_n$  (Table 1) by the molar masses of the repeat units. Assuming that conjugation lengths equal oligomer lengths, theory predicts absorption peaks at 1.21 eV for 19-VTDPP, 1.20 eV for 15-VSeDPP, and 1.92 eV for 31-VPDPP in good agreement with the measured values of 1.29, 1.28, and 2.06 eV. The match of theoretical and experimental spectra shows that theory reproduces the trends correctly and that analysis of the electronic structures provides useful insights.

The large difference in excitation energies of PVPDPP and the other two polymers was attributed to either twisting of the

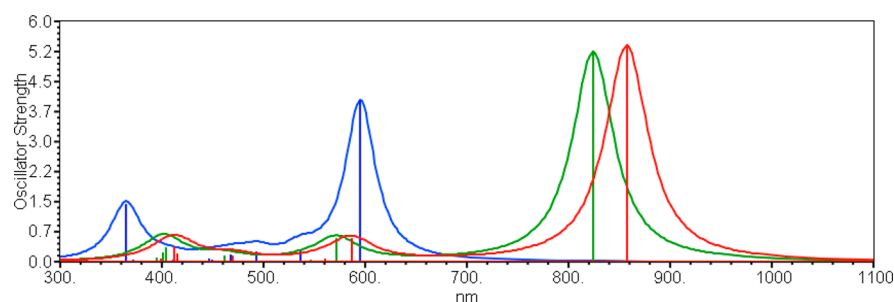


Figure 3. Calculated absorption spectra of 4-VPDPP (blue), 4-VTDPP (green), and 4-VSeDPP (red).

Table 2. Absorption Energies of Dimers through Tetramers and Extrapolated Values for VTDPP, VSeDPP, and VPDPP Oligomers at TDB3P86-30%/6-31G\*

units	VTDPP		VSeDPP		VPDPP	
	eV	nm	eV	nm	eV	nm
2	1.90	651	1.85	670	2.35	5.29
3	1.64	754	1.58	787	2.16	574
4	1.50	825	1.45	858	2.08	596
15			1.20	1003		
19	1.21	984				
31					1.92	643
infinite	1.14	1020	1.12	1047	1.90	650

backbone or higher aromaticity of phenyl compared to thienyl and selenyl groups, as increased aromaticity decreases conjugation along the backbone. The optimized structures of the tetramers in Figure 4 show that all systems are planar

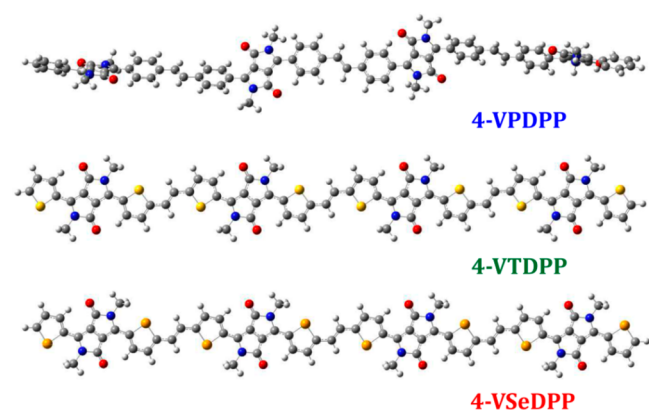


Figure 4. Ground state optimized geometry of the tetramer unit of three copolymers.

around the vinylene moiety. VTDPP and VSeDPP oligomers are entirely planar, and VPDPP oligomers are twisted by  $24^\circ$  between the DPP and phenyl units. The planarization energies of the VPDPP trimer and tetramer are 7.14 and 9.46 kcal/mol, respectively.

The energy changes associated with symmetric rotation between DPP and the donors in D-DPP-D monomer units and for rotation around one of the donor-vinyl single bonds in the V-D-DPP dimers were calculated (Figure 5). All three systems are planar at the donor-vinyl single bond, only phenyl systems are nonplanar between DPP and the phenyl rings.

For both rotations, the barriers are lowest for the phenyl systems. Thienyl and selenyl behave similar at low angles but rotational barriers are higher with selenyl, which indicates that

the selenyl system exhibits the strongest conjugation along the backbone and resists rotational disorder most strongly. These findings rationalize the constant intensity ratio of the high and low energy absorption of PVSeDPP-OD in solution and in the solid state. Nevertheless, the authors also do note that the rotational energy barrier around the DPP-donor bond is higher as compared to the vinyl-donor bond, suggesting the vinyl-donor bond is more susceptible to the torsional disorder in the polymer backbone.

The effect of nonplanarity on the absorption energies was probed by calculating absorption spectra of planar and fully optimized nonplanar 3-VPDPP (Figure 6). The first absorption energy shifts by 30 nm to the red on planarization. The intensity of the low energy absorption decreases slightly, increasing the intensity ratio of low- to high-energy absorption. As the difference in absorption energies of 3-VPDPP and 3-VSeDPP is 213 nm, twisting is not the main reason for the difference in absorption energies.

The extent of conjugation along the backbone can be assessed by comparing the electron densities of the frontier orbitals, as done in Figure 7 for 4-VPDPP and 4-VSeDPP. At first glance, there is no major difference regarding delocalization in HOMOs or LUMOs. On closer inspection, it appears that the contributions of DPP to HOMO and LUMO are somewhat larger in 4-VPDPP, indicating a trend toward localization of the electron density.

Dual band absorption is observed in certain donor–acceptor systems and was shown recently to be associated with the amount of charge transferred during excitation.<sup>49</sup> NBO analysis reveals that the charges on the central DPP units in the ground states are  $-0.105$  e in 4-VPDPP,  $-0.154$  e in 4-VTDPP, and  $-0.165$  e in 4-VSeDPP, confirming the donor–acceptor character of DPP polymers and the larger donor strengths of thienyl and selenyl. The negative charges on DPP are decreased in the first excited states to  $-0.060$  e,  $-0.131$  e, and  $-0.136$  e, respectively. This is in contrast to other donor–acceptor systems involving, for instance, benzothiadiazole (BT),<sup>49</sup> where first excited states involve substantial charge transfer from the donors to BT. For 4-VTDPP and 4-VSeDPP, negative charges on DPP decrease also in the higher excited states, but for 4-VPDPP, the high energy absorption involves charge transfer of 0.018 e from the phenyl-vinylene-phenyl unit to DPP.

Analysis of the electronic configurations involved in the excited states reveals that the first excited states are all dominated by HOMO–LUMO transitions. The strengths of these peaks are explained by the delocalized nature of the HOMOs and LUMOs (Figure 7) and by the small amount of charge transfer involved in the transitions. The higher excited states are consequently weak. The stronger high energy absorption of 4-VPDPP involves a lower lying orbital

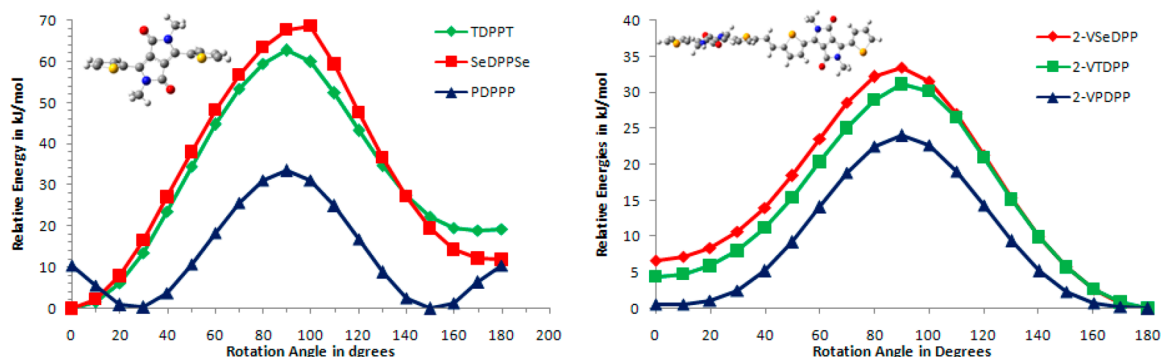


Figure 5. Rotational profiles for rotation around the DPP-donor bonds and the donor-vinyl single bonds in model units (see inset).

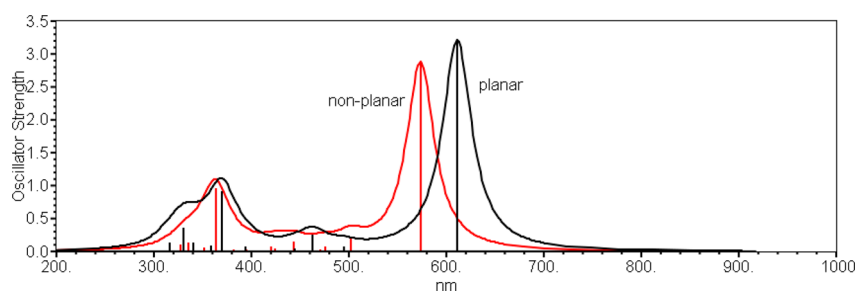


Figure 6. Calculated absorption spectra of planar and nonplanar forms of 3-VPDPP.

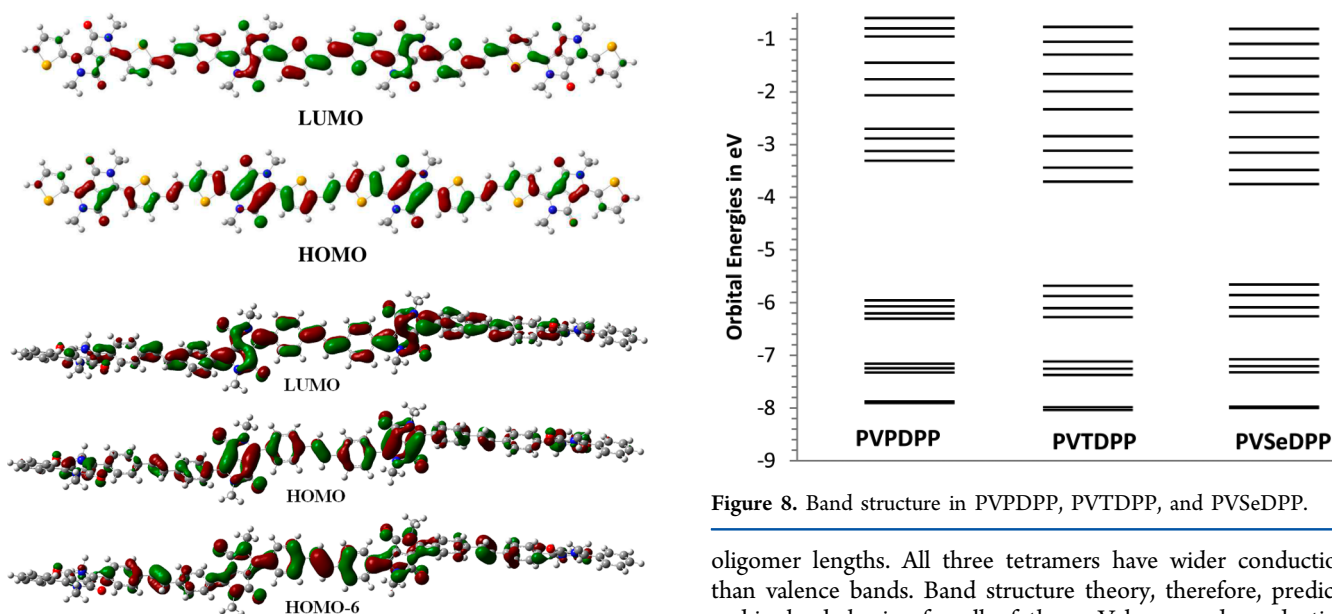


Figure 7. Orbitals of 4-VSeDPP (top) and 4-VPDPP (bottom).

HOMO-6 (Figure 7) and the LUMO and differs therefore from the high energy peaks of BT systems which are dominated by HOMO  $\rightarrow$  LUMO +  $x$  transitions, with  $x$  being the number of repeat units.<sup>49</sup>

To compare the intramolecular transport properties of the three systems, the 10 highest occupied and the 10 lowest unoccupied energy levels of the tetramers are plotted in Figure 8. The four levels lying below the energy gap represent the valence bands of the corresponding polymers; the four levels above the energy gap represent the conduction bands. Using oligomer energy levels as bands is reliable because bandwidths converge very fast toward polymer values with increasing

Figure 8. Band structure in PVPDPP, PVTDPP, and PVSeDPP.

oligomer lengths. All three tetramers have wider conduction than valence bands. Band structure theory, therefore, predicts ambipolar behavior for all of them. Valence and conduction bandwidths are similar for 4-VTDPP and 4-VSeDPP and much wider than for 4-VPDPP. Bands of 4-VSeDPP are slightly wider than for 4-VTDPP and the HOMO of 4-VSeDPP lies a little higher and the LUMO a little lower, in agreement with results from cyclic voltammetry (see below). Thus, the transport is predicted to be best for VSeDPP and worst for PVPDPP.

In summary, theory predicts very similar properties for VTDPP and VSeDPP oligomers, with slightly better values for the latter. VPDPP has the largest band gap and the smallest bandwidths. Therefore, PVSeDPP should perform best of the three systems in terms of conductivity and light absorption, although the improvement over PVTDPP is expected to be small. For the optical and electrochemical properties, theory and experiment are in perfect agreement, but transport properties of PVSeDPP have so far not matched those of

PVTDPP. The present theoretical analysis excludes electronic properties at the single particle level as the reason for the poorer transport properties of PVSeDPP compared to PVTDP. A possible contribution could be the lower molecular weight and therefore shorter oligomer lengths. As shown below, there are also differences in morphology between the two systems, which are not considered in the present theoretical analysis.

**2.4. Electrochemical Properties.** Electrochemical properties were determined by cyclic voltammetry. The positions of the HOMO and LUMO were calculated from the corresponding oxidation and reduction potentials, respectively, and band gaps were measured by taking the difference between the energy levels of the frontier molecular orbitals. The cyclic voltammograms of the three polymers are shown in Figure 9.

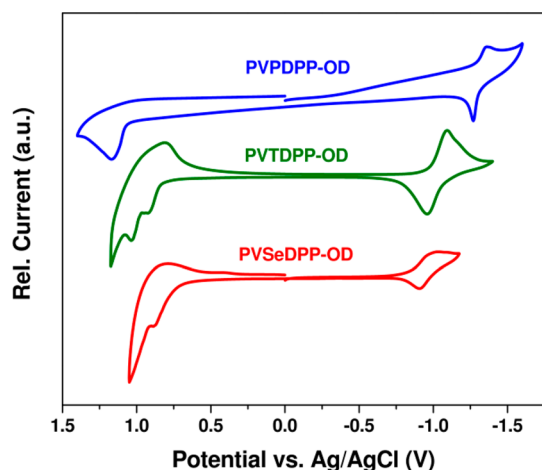


**Figure 9.** Cyclic voltammograms of three DPP based vinylene polymers recorded at a scan rate of 0.1 V/s.

The oxidation onset of PVPDPP-OD, PVTDP-OD, and PVSeDPP-OD is at 1.07, 0.87, and 0.75 V, respectively, corresponding to the HOMO energy level of  $-5.57$ ,  $-5.37$ , and  $-5.25$  eV. PVPDPP-OD, PVTDP-OD, and PVSeDPP-OD exhibit LUMO energy levels at  $-3.22$ ,  $-3.56$ , and  $-3.69$  eV, which were calculated from their reduction onset at  $-1.28$ ,  $-0.94$ , and  $-0.81$  V, respectively. Inclusion of chalcogen atoms reduces the band gap, and the decrease is largest for the selenium-containing polymer. Improved coupling between donor and acceptor units raises the HOMO energy of chalcogen-based polymers, and the stronger donating strength of selenophene is responsible for the highest lying HOMO of PVSeDPP-OD. On the other side, the lower electron affinity of selenium stabilizes the LUMO as compared to the other two polymers, which is a characteristic for the selenium containing functional materials.<sup>50,51</sup> Hence, by comparing the cyclic voltammograms of the three polymers, we can conclude that chalcogen atoms affect LUMO energy levels to a greater extent than HOMO levels. Theoretical calculations predict the same.

All three polymers showed a reversible reduction cycle, but the oxidation scan was irreversible in nature. The HOMO and LUMO energies and corresponding band gaps are summarized in Table 3. We see a gradual reduction in electrochemical band gap in these three DPP polymers similar to their optical band gap. We also observed the difference between the band gap measured in optical and electrochemical studies, which is attributed to the exciton binding energy.

**Table 3. Summary of Optical and Electrochemical Data of the Three Copolymers**

polymer	UV-vis absorption spectra			electrochemical properties		
	solution	thin film	$E_g^{\text{opt } a}$ (eV)	HOMO (eV)	LUMO (eV)	$E_g^{\text{elec}}$ (eV)
	$\lambda_{\text{max}}$ (nm)	$\lambda_{\text{max}}$ (nm)				
PVPDPP-OD	530	536	2.06	$-5.57$	$-3.22$	2.35
PVTDP-OD	762	788	1.29	$-5.37$	$-3.56$	1.81
PVSeDPP-OD	765	809	1.28	$-5.22$	$-3.69$	1.56

<sup>a</sup>Calculated from onset of solution state absorption spectra.

**2.5. Charge Transport Properties.** The charge transport properties of the copolymers were evaluated using thin film transistor (TFT) measurements. Charge transport behavior in this class of materials is directly related to their electronic and solid-state packing properties. TFTs were fabricated in two different device geometries, namely, bottom-gate bottom-contact (BG-BC) and top-gate bottom-contact (TG-BC). In BG-BC devices, Au source-drain electrodes were patterned over Si/SiO<sub>2</sub> substrates where Si and SiO<sub>2</sub> acted as the gate electrode and the gate dielectric layer, respectively. TG-BC devices were made on glass substrates using prepatterned bilayer Au/Al source and drain electrodes. A fluoropolymer, CYTOP (Ashai glass), and Al were used as the dielectric and gate electrode materials, respectively. Polymer films were spin-coated and annealed at 140 °C in a nitrogen atmosphere.

For both PVTDP-OD and PVSeDPP-OD, improved charge transport characteristics were observed in the TG-BC device geometry with both polymers exhibiting ambipolar behavior. The output characteristics in both the p- and n-channel operating regimes are shown in Figure 10. All devices show good channel current saturation with minimum hysteresis in forward and reverse biasing. The performance characteristics of the different polymer transistors are summarized in Table 4.

Though both of the polymers showed ambipolar transport character, the hole ( $\mu_h$ ) mobility was significantly higher than the electron mobility ( $\mu_e$ ). Overall, the PVTDP-OD polymer showed better charge carrier mobility compared to its selenium analogue. The highest hole mobility observed for PVTDP-OD was  $0.1 \text{ cm}^2 \text{ V}^{-1} \text{ s}^{-1}$ , while it reduced to half that value for PVSeDPP-OD ( $0.05 \text{ cm}^2 \text{ V}^{-1} \text{ s}^{-1}$ ). Electron mobilities are lower, 0.05 and  $0.005 \text{ cm}^2 \text{ V}^{-1} \text{ s}^{-1}$  for PVTDP-OD and PVSeDPP-OD, respectively. Furthermore, the threshold voltages ( $V_{\text{Th}}$ ) measured for p- and n-channel operations were significantly high indicative of the presence of a large number of trap states at the semiconductor–dielectric interface. Use of an alternative gate dielectric and/or improvements in the polymer processing could lead to reduced  $V_{\text{Th}}$ . However, this is beyond the scope of this study and will be the focus of future investigations.

For a similar polymer (2DPP-OD-OD), as mentioned previously, with repetitive 2-octyldecyl alkyl chains on the DPP monomers without any vinyl linkage, no field effect mobility was observed.<sup>48</sup> Hence, close proximity of a very long and branched alkyl chain appears to be detrimental for molecular packing and consequently for measurable charge transport in the device channel. Here the vinylene group acts as a spacer between two DPP units to reduce the interchain repulsive interaction. Additionally, vinylene units increase the donating strength to improve the push pull–interaction in D–A copolymers enhancing the p-channel mobility.<sup>6,36,52–55</sup> Thus,

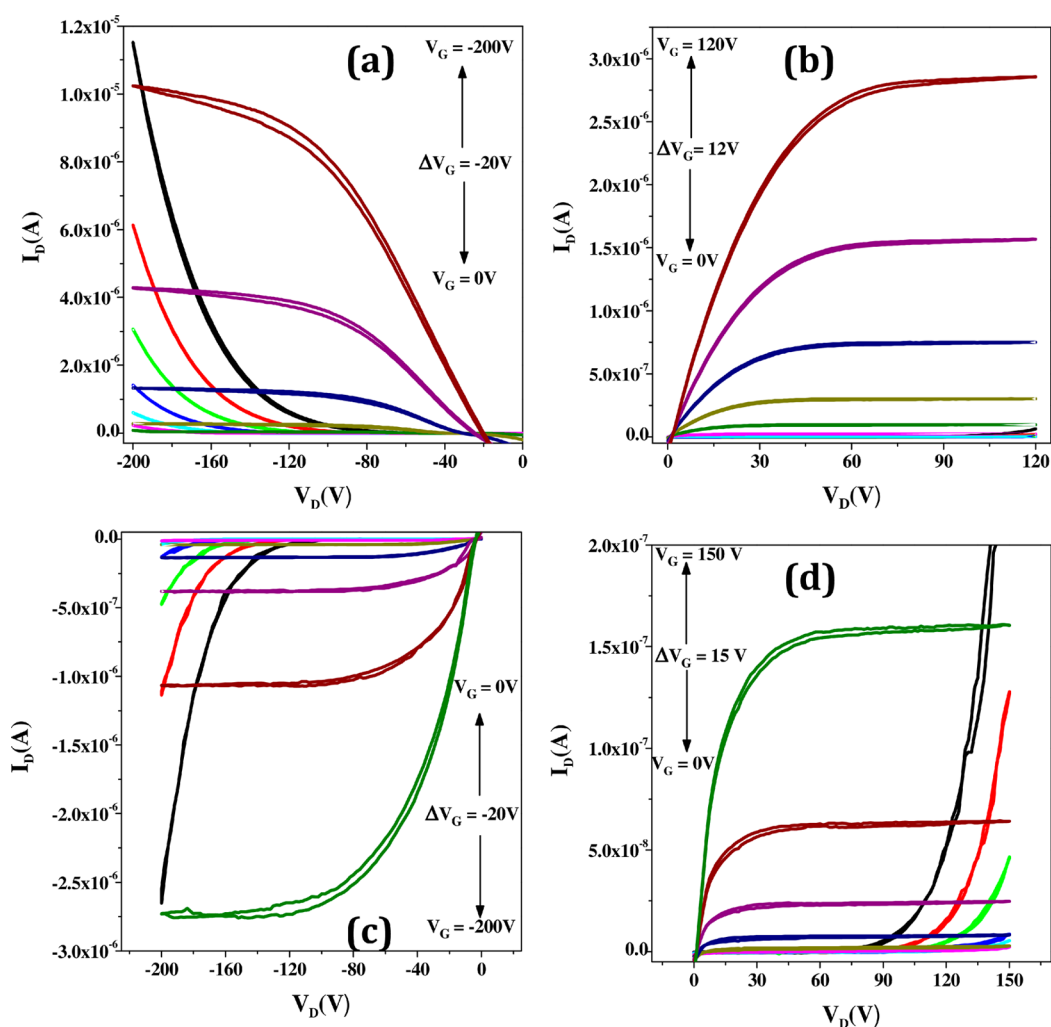


**Figure 10.** p-Channel (a, c) and n-channel (b, d) output characteristics of OFET devices fabricated from PVTDPP-OD (a, b) and PVSeDPP-OD (c, d).

**Table 4. Summary of the OFET Device Parameters for the Two Chalcogen Based Copolymers in the TG-BC Device Configuration**

polymer	D/S	gate dielectric	$\mu_e$ (cm <sup>2</sup> V <sup>-1</sup> s <sup>-1</sup> )	$\mu_h$ (cm <sup>2</sup> V <sup>-1</sup> s <sup>-1</sup> )	$V_{Th}$ (V)	
					(n)	(p)
PVTDPP-OD	Au/Al	CYTOP	0.05	0.1	74	-143
PVSeDPP-OD	Au/Al	CYTOP	0.005	0.05	141	-144

by increasing the number of thiophene or selenophene groups as spacers in DPP based polymers with very long alkyl chains, a significantly higher charge carrier mobility is obtained.<sup>28,43</sup> In a similar way, by reducing the steric repulsion with the incorporation of shorter alkyl chains (2-hexyldecyl) in TDPP vinylene polymers, Wu et al. have demonstrated a similar charge carrier mobility as in the present work with low threshold voltages<sup>36</sup> which indicates a decrease in the interfacial defects.

**2.6. Near Edge X-ray Absorption Spectroscopy.** The extent of molecular ordering in 150 nm thin films of PVTDPP-OD and PVSeDPP-OD was investigated using near-edge X-ray absorption fine structure (NEXAFS) measurements in transmission mode at the Pollux<sup>56</sup> beamline at Swiss Light Source (SLS). To avoid any X-ray induced damage, a defocused beam was used to obtain carbon K-edge spectra with a low dwell time. Samples were also measured after annealing at 200 °C for

30 min. As shown in Figure 11, a distinct peak at 284.6 eV is seen for all of the samples (except for the as-cast PVTDPP-OD). We are chiefly concerned with this peak, since it is sensitive to the orientation of the aromatic structures of the polymer backbone. The peak corresponds to the C 1s →  $\pi^*$  transition primarily arising from the aromatic component in the samples. The intensity of this peak depends on the cosine of the angle between the transition dipole moment (TDM) and the electric field vector (**E**) of the incident radiation.<sup>57</sup> The TDM in the case of the polymers such as those under investigation in this study is perpendicular to the conjugation plane of the aromatic components. Since the incident **E** vector lies in the plane of the sample, due to the linear horizontal polarization of the X-ray radiation, the intensity of this resonance peak is at the maximum if the aromatic rings are aligned on the sample in an edge-on fashion with the polymer backbone also perpendicular to the **E** vector. While variation in

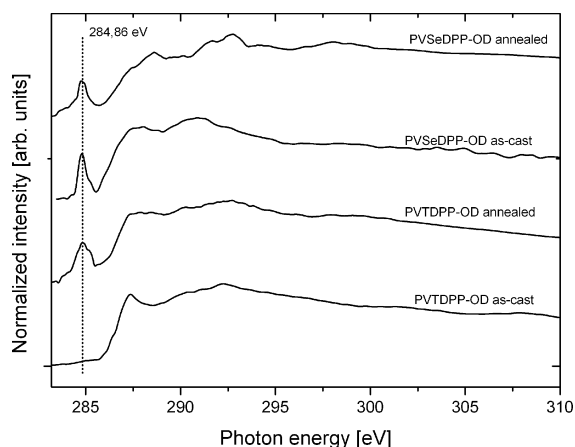


**Figure 11.** Averaged and normalized NEXAFS spectra of as-cast and annealed thin film samples of PVSeDPP-OD and PVTDDP-OD.

this intensity can indicate the local alignment of the aromatic rings with respect to the sample surface, one can also comment on the extent of ordering if spectra are averaged over a large area. Several spectra were obtained over a region of  $200\ \mu\text{m}$  in order to choose a smaller representative region of the sample. Line spectra over a  $20\ \mu\text{m}$  length were obtained before and after annealing without changing the orientation and relative position of the sample with respect to the incident radiation. As can be seen in Figure 11, there is a significant difference between the spectra of the as-cast and annealed samples in the case of PVTDDP-OD. The orientation of the aromatic rings can be considered to be isotropic in the case of as-cast PVTDDP-OD, since the resonance peak is insignificant. The intensity of the resonance peak increases upon annealing, indicating that the aromatic rings prefer a particular orientation in the chosen area of investigation. This also indicates that the molecular ordering is enhanced upon annealing. This behavior is not observed in the spectra of PVSeDPP-OD. The degree of molecular ordering does not change significantly upon annealing, thus indicating that the film is sufficiently ordered even before annealing. However, contrary to these findings, the charge transport properties of PVTDDP-OD are better than those of PVSeDPP-OD. This indicates that the differences in molecular ordering between these two polymers are not the reason for the inferior charge transport properties of PVSeDPP-OD. The authors do note that definitive comments on the molecular tilt and orientation require further detailed investigations.

### 3. CONCLUSION

Optical properties of the vinylene-DPP polymers follow similar trends as observed for the DPP based nonvinylene polymers; optical band gaps gradually decrease with the increase in the donating strength from phenyl to selenyl, and selenyl yields a broader optical absorption than thienyl. The vinylene unit leads to a slight increase in the optical band gap but improves order in the solid state.

Theoretical analysis reveals that only PVPDPP oligomers have nonplanar structures. Twisting along the backbone increases the absorption energy, but the major contribution to the much higher excitation energies of PVPDPP compared to PVTDDP and PVSeDPP is electronic effects of the phenyl ring.

Optical, electrochemical, and NEXAFS experiments and theory predict better transport properties for PVSeDPP than for PVTDDP. However, OFET measurements achieved slightly lower p- and n-channel mobilities with PVSeDPP. A possible reason for the inferior performance of PVSeDPP is the lower molecular weight of PVSeDPP, which corresponds to an average chain length of 15 repeat units as compared to 19 repeat units for PVTDDP. We hope to improve device performance in the future by better controlling crystallinity, orientation of the polymer chain over the substrates, and/or processing of the thin film during device fabrication.

## ■ ASSOCIATED CONTENT

### 📄 Supporting Information

Experimental details regarding synthesis of monomers and copolymers with their characterization and  $^1\text{H}$  and  $^{13}\text{C}$  NMR spectra. The Supporting Information is available free of charge on the ACS Publications website at DOI: 10.1021/acs.jpcc.5b03145.

## ■ AUTHOR INFORMATION

### Corresponding Author

\*Phone: +91-80-22932651. Fax: +91-80-23601310. E-mail: satish@sscu.iisc.ernet.in.

### Notes

The authors declare no competing financial interest.

## ■ ACKNOWLEDGMENTS

J.D. and T.M. acknowledge Council of Scientific and Industrial Research (CSIR) for a senior research fellowship (SRF). S.P. acknowledge a research grant from the Ministry of Communication and Information Technology under the Centre of Excellence in Nanoelectronics, Phase II and British Council through the UK-India Education and Research Initiative (UKIERI) programme. We acknowledge the Paul Scherrer Institut, Villigen, Switzerland, for provision of synchrotron radiation beamtime at the PolLux beamline of the SLS and would like to thank Dr. Benjamin Watts for assistance. The PolLux end station was financed by the German Minister für Bildung und Forschung (BMBF) through contracts 05KS4WE1/6 and 05KS7WE1.

## ■ REFERENCES

- Burroughes, J. H.; Bradley, D. D. C.; Brown, A. R.; Marks, R. N.; Mackay, K.; Friend, R. H.; Burn, P. L.; Holmes, A. B. Light-Emitting Diodes Based on Conjugated Polymers. *Nature* **1990**, *347*, 539–541.
- Morgado, J.; Friend, R. H.; Cacialli, F. Improved Efficiency of Light-Emitting Diodes Based on Polyfluorene Blends upon Insertion of a Poly(p-phenylene vinylene) Electron-Confinement Layer. *Appl. Phys. Lett.* **2002**, *80*, 2436–2438.
- Braun, D.; Heeger, A. J. Visible-Light Emission from Semiconducting Polymer Diodes. *Appl. Phys. Lett.* **1991**, *58*, 1982–1984.
- Tajima, K.; Suzuki, Y.; Hashimoto, K. Polymer Photovoltaic Devices using Fully Regioregular Poly(2-methoxy-5-(3',7'-dimethyloctyloxy))-1,4-phenylenevinylene. *J. Phys. Chem. C* **2008**, *112*, 8507–8510.
- Blayney, A. J.; Perepichka, I. F.; Wudl, F.; Perepichka, D. F. Advances and Challenges in the Synthesis of Poly(p-phenylene vinylene)-Based Polymers. *Isr. J. Chem.* **2014**, *54*, 674–688.
- Kim, J.; Baeg, K.-J.; Khim, D.; James, D. T.; Kim, J.-S.; Lim, B.; Yun, J.-M.; Jeong, H.-G.; Amegadze, P. S. K.; Noh, Y.-Y.; et al. Optimal Ambipolar Charge Transport of Thienylenevinylene-Based Polymer Semiconductors by Changes in Conformation for High-Performance



Organic Thin Film Transistors and Inverters. *Chem. Mater.* **2013**, *25*, 1572–1583.

(7) Li, H.; Liu, F.; Wang, X.; Gu, C.; Wang, P.; Fu, H. Diketopyrrolopyrrole-Thiophene-Benzothiadiazole Random Copolymers: An Effective Strategy To Adjust Thin-Film Crystallinity for Transistor and Photovoltaic Properties. *Macromolecules* **2013**, *46*, 9211–9219.

(8) Henckens, A.; Colladet, K.; Fourier, S.; Cleij, T. J.; Lutsen, L.; Gelan, J.; Vanderzande, D. Synthesis of 3,4-diphenyl-Substituted Poly(thienylene vinylene) Low-Band-Gap Polymers via the Dithiocarbamate Route. *Macromolecules* **2005**, *38*, 19–26.

(9) Al-Hashimi, M.; Baklar, M. A.; Colleaux, F.; Watkins, S. E.; Anthopoulos, T. D.; Stingelin, N.; Heeney, M. Synthesis, Characterization, and Field Effect Transistor Properties of Regioregular Poly(3-alkyl-2,5-selenylenevinylene). *Macromolecules* **2011**, *44*, 5194–5199.

(10) Fuchigami, H.; Tsumura, A.; Koezuka, H. Polythienylenevinylene Thin-Film-Transistor With High Carrier Mobility. *Appl. Phys. Lett.* **1993**, *63*, 1372–1374.

(11) Brown, A. R.; Jarrett, C. P.; deLeeuw, D. M.; Matters, M. Field-Effect Transistors Made from Solution-Processed Organic Semiconductors. *Synth. Met.* **1997**, *88*, 37–55.

(12) Huo, L.; Chen, T. L.; Zhou, Y.; Hou, J.; Chen, H.-Y.; Yang, Y.; Li, Y. Improvement of Photoluminescent and Photovoltaic Properties of Poly(thienylene vinylene) by Carboxylate Substitution. *Macromolecules* **2009**, *42*, 4377–4380.

(13) Wan, M.; Wu, W.; Sang, G.; Zou, Y.; Liu, Y.; Li, Y. Poly(thienylene-vinylene-thienylene) with Cyano Substituent: Synthesis and Application in Field-Effect Transistor and Polymer Solar Cell. *J. Polym. Sci., Part A: Polym. Chem.* **2009**, *47*, 4028–4036.

(14) Musser, A. J.; Al-Hashimi, M.; Maiuri, M.; Brida, D.; Heeney, M.; Cerullo, G.; Friend, R. H.; Clark, J. Activated Singlet Exciton Fission in a Semiconducting Polymer. *J. Am. Chem. Soc.* **2013**, *135*, 12747–12754.

(15) Lafalce, E.; Jiang, X.; Zhang, C. Generation and Recombination Kinetics of Optical Excitations in Poly(3-dodecylthienylenevinylene) with Controlled Regioregularity. *J. Phys. Chem. B* **2011**, *115*, 13139–13148.

(16) Neef, C. J.; Ferraris, J. P. MEH-PPV: Improved Synthetic Procedure and Molecular Weight Control. *Macromolecules* **2000**, *33*, 2311–2314.

(17) Osaka, I.; McCullough, R. D. Advances in Molecular Design and Synthesis of Regioregular Polythiophenes. *Acc. Chem. Res.* **2008**, *41*, 1202–1214.

(18) Zhang, C.; Sun, J.; Li, R.; Sun, S.-S.; Lafalce, E.; Jiang, X. Poly(3-dodecylthienylenevinylene)s: Regioregularity and Crystallinity. *Macromolecules* **2011**, *44*, 6389–6396.

(19) Junkers, T.; Vandenbergh, J.; Adriaensens, P.; Lutsen, L.; Vanderzande, D. Synthesis of Poly(p-phenylene vinylene) Materials via the Precursor Routes. *Polym. Chem.* **2012**, *3*, 275–285.

(20) Schwartz, B. J. Conjugated Polymers as Molecular Materials: How Chain Conformation and Film Morphology Influence Energy Transfer and Interchain Interactions. *Annu. Rev. Phys. Chem.* **2003**, *54*, 141–172.

(21) Nayyar, I. H.; Batista, E. R.; Tretiak, S.; Saxena, A.; Smith, D. L.; Martin, R. L. Effect of trans- and cis-Isomeric Defects on the Localization of the Charged Excitations in  $\pi$ -Conjugated Organic Polymers. *J. Polym. Sci., Part B: Polym. Phys.* **2013**, *51*, 935–942.

(22) Hu, D. H.; Yu, J.; Wong, K.; Bagchi, B.; Rossky, P. J.; Barbara, P. F. Collapse of Stiff Conjugated Polymers with Chemical Defects into Ordered, Cylindrical Conformations. *Nature* **2000**, *405*, 1030–1033.

(23) Hwang, I.; Scholes, G. D. Electronic Energy Transfer and Quantum-Coherence in  $\pi$ -Conjugated Polymers. *Chem. Mater.* **2011**, *23*, 610–620.

(24) Wong, K. F.; Skaf, M. S.; Yang, C. Y.; Rossky, P. J.; Bagchi, B.; Hu, D. H.; Yu, J.; Barbara, P. F. Structural and Electronic Characterization of Chemical and Conformational Defects in Conjugated Polymers. *J. Phys. Chem. B* **2001**, *105*, 6103–6107.

(25) Bolinger, J. C.; Traub, M. C.; Brazard, J.; Adachi, T.; Barbara, P. F.; Vanden Bout, D. A. Conformation and Energy Transfer in Single Conjugated Polymers. *Acc. Chem. Res.* **2012**, *45*, 1992–2001.

(26) Yuen, J. D.; Fan, J.; Seifert, J.; Lim, B.; Hufschmid, R.; Heeger, A. J.; Wudl, F. High Performance Weak Donor-Acceptor Polymers in Thin Film Transistors: Effect of the Acceptor on Electronic Properties, Ambipolar Conductivity, Mobility, and Thermal Stability. *J. Am. Chem. Soc.* **2011**, *133*, 20799–20807.

(27) Bronstein, H.; Chen, Z. Y.; Ashraf, R. S.; Zhang, W. M.; Du, J. P.; Durrant, J. R.; Tuladhar, P. S.; Song, K.; Watkins, S. E.; Geerts, Y.; et al. Thieno[3,2-b]thiophene-Diketopyrrolopyrrole-Containing Polymers for High-Performance Organic Field-Effect Transistors and Organic Photovoltaic Devices. *J. Am. Chem. Soc.* **2011**, *133*, 3272–3275.

(28) Kang, I.; Yun, H.-J.; Chung, D. S.; Kwon, S.-K.; Kim, Y.-H. Record High Hole Mobility in Polymer Semiconductors via Side-Chain Engineering. *J. Am. Chem. Soc.* **2013**, *135*, 14896–14899.

(29) Kanimozhi, C.; Yaacobi-Gross, N.; Chou, K. W.; Amassian, A.; Anthopoulos, T. D.; Patil, S. Diketopyrrolopyrrole-Diketopyrrolopyrrole-Based Conjugated Copolymer for High-Mobility Organic Field-Effect Transistors. *J. Am. Chem. Soc.* **2012**, *134*, 16532–16535.

(30) Lee, J.; Han, A. R.; Yu, H.; Shin, T. J.; Yang, C.; Oh, J. H. Boosting the Ambipolar Performance of Solution-Processable Polymer Semiconductors via Hybrid Side-Chain Engineering. *J. Am. Chem. Soc.* **2013**, *135*, 9540–9547.

(31) Li, W. W.; Furlan, A.; Hendriks, K. H.; Wienk, M. M.; Janssen, R. A. J. Efficient Tandem and Triple-Junction Polymer Solar Cells. *J. Am. Chem. Soc.* **2013**, *135*, 5529–5532.

(32) Lee, J.; Han, A. R.; Kim, J.; Kim, Y.; Oh, J. H.; Yang, C. Solution-Processable Ambipolar Diketopyrrolopyrrole-Selenophene Polymer with Unprecedentedly High Hole and Electron Mobilities. *J. Am. Chem. Soc.* **2012**, *134*, 20713–20721.

(33) Sun, B.; Hong, W.; Yan, Z.; Aziz, H.; Li, Y. Record High Electron Mobility of  $6.3 \text{ cm}^2 \text{ V}^{-1} \text{ s}^{-1}$  Achieved for Polymer Semiconductors Using a New Building Block. *Adv. Mater.* **2014**, *26*, 2636–2642.

(34) You, J. B.; Dou, L. T.; Yoshimura, K.; Kato, T.; Ohya, K.; Moriarty, T.; Emery, K.; Chen, C. C.; Gao, J.; Li, G. et al. A Polymer Tandem Solar Cell with 10.6% Power Conversion Efficiency. *Nat. Commun.* **2013**, *4*.

(35) Dou, L. T.; Chang, W. H.; Gao, J.; Chen, C. C.; You, J. B.; Yang, Y. A Selenium-Substituted Low-Bandgap Polymer with Versatile Photovoltaic Applications. *Adv. Mater.* **2013**, *25*, 825–831.

(36) Wu, P.-T.; Kim, F. S.; Jenekhe, S. A. New Poly(arylene vinylene)s Based on Diketopyrrolopyrrole for Ambipolar Transistors. *Chem. Mater.* **2011**, *23*, 4618–4624.

(37) Yun, H.-J.; Choi, H. H.; Kwon, S.-K.; Kim, Y.-H.; Cho, K. Conformation-Insensitive Ambipolar Charge Transport in a Diketopyrrolopyrrole-Based Co-polymer Containing Acetylene Linkages. *Chem. Mater.* **2014**, *26*, 3928–3937.

(38) Sonar, P.; Zhuo, J.-M.; Zhao, L.-H.; Lim, K.-M.; Chen, J.; Rondinone, A. J.; Singh, S. P.; Chua, L.-L.; Ho, P. K. H.; Dodabalapur, A. Furan Substituted Diketopyrrolopyrrole and Thienylenevinylene Based Low Band Gap Copolymer for High Mobility Organic Thin Film Transistors. *J. Mater. Chem.* **2012**, *22*.

(39) Ha, T.-J.; Sonar, P.; Dodabalapur, A. Charge Transport Study of High Mobility Polymer Thin-Film Transistors Based on Thiophene Substituted Diketopyrrolopyrrole Copolymers. *Phys. Chem. Chem. Phys.* **2013**, *15*, 9735–9741.

(40) Chen, H. J.; Guo, Y. L.; Yu, G.; Zhao, Y.; Zhang, J.; Gao, D.; Liu, H. T.; Liu, Y. Q. Highly  $\pi$ -Extended Copolymers with Diketopyrrolopyrrole Moieties for High-Performance Field-Effect Transistors. *Adv. Mater.* **2012**, *24*, 4618–4622.

(41) Han, A. R.; Dutta, G. K.; Lee, J.; Lee, H. R.; Lee, S. M.; Ahn, H.; Shin, T. J.; Oh, J. H.; Yang, C.  $\epsilon$ -Branched Flexible Side Chain Substituted Diketopyrrolopyrrole-Containing Polymers Designed for High Hole and Electron Mobilities. *Adv. Funct. Mater.* **2015**, *25*, 247–254.

(42) Back, J. Y.; Yu, H.; Song, I.; Kang, I.; Ahn, H.; Shin, T. J.; Kwon, S. K.; Oh, J. H.; Kim, Y. H. Investigation of Structure–Property Relationships in Diketopyrrolopyrrole-Based Polymer Semiconductors via Side-Chain Engineering. *Chem. Mater.* **2015**, *27*, 1732–1739.

(43) Kang, I.; An, T. K.; Hong, J. A.; Yun, H. J.; Kim, R.; Chung, D. S.; Park, C. E.; Kim, Y. H.; Kwon, S. K. Effect of Selenophene in a DPP Copolymer Incorporating a Vinyl Group for High-Performance Organic Field-Effect Transistors. *Adv. Mater.* **2013**, *25*, 524–528.

(44) Yun, H. J.; Kang, S.-J.; Xu, Y.; Kim, S. O.; Kim, Y. H.; Noh, Y.-Y.; Kwon, S. K. Dramatic Inversion of Charge Polarity in Diketopyrrolopyrrole-Based Organic Field-Effect Transistors via a Simple Nitrile Group Substitution. *Adv. Mater.* **2014**, *26*, 7300–7307.

(45) Yun, H. J.; Choi, H. H.; Kwon, S. K.; Kim, Y. H.; Cho, K. Polarity Engineering of Conjugated Polymers by Variation of Chemical Linkages Connecting Conjugated Backbones. *ACS Appl. Mater. Interfaces* **2015**, *7*, 5898–5906.

(46) Dhar, J.; Venkatramaiah, N.; A, A.; Patil, S. Photophysical, Electrochemical and Solid State Properties of Diketopyrrolopyrrole Based Molecular Materials: Importance of the Donor Group. *J. Mater. Chem. C* **2014**, *2*, 3457–3466.

(47) Mizuguchi, J.; Grubenmann, A.; Wooden, G.; Rihs, G. Structures of 3,6-diphenylpyrrolo [3,4-*c*]pyrrole-1,4-dione and 2,5-dimethyl-3,6-diphenylpyrrolo[3,4-*c*]pyrrole-1,4-dione. *Acta Crystallogr., Sect. B: Struct. Sci.* **1992**, *48*, 696–700.

(48) Kanimozhi, C.; Yaacobi-Gross, N.; Burnett, E. K.; Briseno, A. L.; Anthopoulos, T. D.; Salzner, U.; Patil, S. Use of Side-Chain for Rational Design of n-type Diketopyrrolopyrrole-Based Conjugated Polymers: What did We Find out? *Phys. Chem. Chem. Phys.* **2014**, *16*, 17253–17265.

(49) Salzner, U. Effect of Donor-Acceptor Substitution on Optoelectronic Properties of Conducting Organic Polymers. *J. Chem. Theory Comput.* **2014**, *10*, 4921–4937.

(50) Gibson, G. L.; McCormick, T. M.; Seferos, D. S. Atomistic Band Gap Engineering in Donor–Acceptor Polymers. *J. Am. Chem. Soc.* **2011**, *134*, 539–547.

(51) Villar, H. O.; Otto, P.; Dupuis, M.; Ladik, J. Ab-Initio and Electron Correlation Corrected Energy-Band Structure of Polymeric 5-Membered Heterocycles. *Synth. Met.* **1993**, *59*, 97–110.

(52) Jeeva, S.; Lukoyanova, O.; Karas, A.; Dadvand, A.; Rosei, F.; Perepichka, D. F. Highly Emissive and Electrochemically Stable Thienylene Vinylene Oligomers and Copolymers: An Unusual Effect of Alkylsulfanyl Substituents. *Adv. Funct. Mater.* **2010**, *20*, 1661–1669.

(53) Fu, Y.; Cheng, H.; Elsenbaumer, R. L. Electron-Rich Thienylene–Vinylene Low Bandgap Polymers. *Chem. Mater.* **1997**, *9*, 1720–1724.

(54) Zhao, C.; Li, C.; Ma, Y.; Zhao, C.; Wang, W. Theoretical Investigation into Electronic Structures and Charge Transfer Properties of  $\pi$ -Conjugated System with Different Combinations of Thiophene and Vinyl/Butadiene. *Chin. J. Chem.* **2012**, *30*, 2501–2508.

(55) Lim, B.; Baeg, K.-J.; Jeong, H.-G.; Jo, J.; Kim, H.; Park, J.-W.; Noh, Y.-Y.; Vak, D.; Park, J.-H.; Park, J.-W.; et al. A New Poly(thienylenevinylene) Derivative with High Mobility and Oxidative Stability for Organic Thin-Film Transistors and Solar Cells. *Adv. Mater.* **2009**, *21*, 2808–2814.

(56) Raabe, J.; Tzvetkov, G.; Flechsig, U.; Böge, M.; Jaggi, A.; Sarafimov, B.; Vernooij, M. G. C.; Huthwelker, T.; Ade, H.; Kilcoyne, D.; Tyliszczak, T.; et al. PoLux: A New Facility for Soft X-Ray Spectromicroscopy at the Swiss Light Source. *Rev. Sci. Instrum.* **2008**, *79*, 113704.

(57) Stöhr, J. *NEXAFS Spectroscopy*; Springer-Verlag: Berlin, 1992.